Regenerative Electronic Biosensors Using Supramolecular Approaches

Xuexin Duan,[†] Nitin K. Rajan,[‡] David A. Routenberg,[†] Jurriaan Huskens,[§] and Mark A. Reed[†,‡,*]

[†]Department of Electrical Engineering, Yale University, New Haven, Connecticut 06520, United States, [‡]Department of Applied Physics, Yale University, New Haven, Connecticut 06520, United States, and [§]Molecular Nanofabrication Group, MESA+ Institute for Nanotechnology, University of Twente, P.O. Box 217, 7500 AE Enschede, The Netherlands

ABSTRACT A supramolecular interface for Si nanowire FETs has been developed with the aim of creating regenerative electronic biosensors. The key to the approach is Si-NWs functionalized with β-cyclodextrin (β-CD), to which receptor moieties can be attached with an orthogonal supramolecular linker. Here we demonstrate full recycling using the strongest biomolecular system known, streptavidin (SAv)—biotin. The bound SAv and the linkers can be selectively removed from the surface through competitive desorption with concentrated β-CD, regenerating the sensor for repeated use. An added advantage of β-CD is the possibility of stereoselective sensors, and we demonstrate here the ability to quantify the enantiomeric composition of chiral targets.

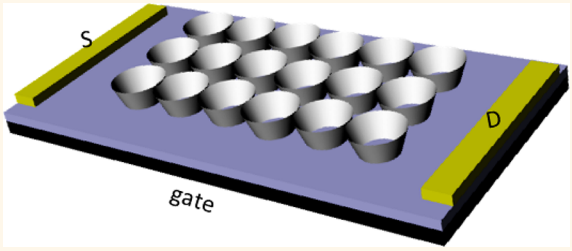

KEYWORDS: silicon nanowire · supramolecular chemistry · biosensor · stereoselective sensor

In recent years, there has been a surge of interest in exploiting biosensing systems based on CMOS-compatible silicon nanowire field-effect transistors (NWFETs).[1−4] Si-NWs modified with specific surface receptors present a powerful detection platform for a broad range of biological and chemical species. The small diameter of NWFET devices provides extremely high sensitivity because the binding of target molecules causes accumulation/depletion of carriers throughout the wire cross-section, enabling label-free real-time detection and monitoring of biomolecular interactions.[5−14] Although such devices were first demonstrated by chemically synthesized VLS NWs,[11] top-down fabricated CMOS-compatible Si-NW devices offer advantages of high yield, exceptional uniformity, and system-level integration and multiplexing.[12] Within the past few years, many of the previous limitations to charge-based affinity sensors, such as charge screening and sensor drift, have been solved.[15−17] In addition, the ability to multiplex electronic sensors for higher accuracy and false positive/negative elimination has become an attractive benefit of the approach. NWFETs not only represent an attractive technology for future miniaturized and multiplexed biosensing platforms but could also be extended to high-throughput functional assays (*e.g.*, drug screening).

In order to detect bimolecular interactions, receptor molecules (*e.g.*, proteins or protein-binding ligands) are immobilized on the Si NWFET surface, and the target (bio)molecules are recognized through specific binding. The performance of biosensors, specifically the sensitivity, specificity, reusability, chemical stability, and reproducibility, is critically dependent on the (bio)-functionalization of the sensor platform. The type of linkers used for the immobilization of the capture probes and the exact immobilization protocols play a vital role in the overall performance of sensors.[18] Currently, the commonly used strategy is attaching the receptor molecules to the nanowire surface *via* a covalent approach through amino silanization of the Si/SiO_2 surface, followed by amine coupling.[4,19] Such covalent attachment has disadvantages, such as autoxidation of amine-functionalized surfaces, which could limit long-term device application, lack of control of molecule placement and conformation (with a potential reduction in activity), and increasing heterogeneity in the population of immobilized species. Most importantly, such attachment is irreversible, and functionalized devices can

* Address correspondence to mark.reed@yale.edu.

Received for review December 30, 2012 and accepted April 1, 2013.

Published online April 02, 2013
10.1021/nn306034f

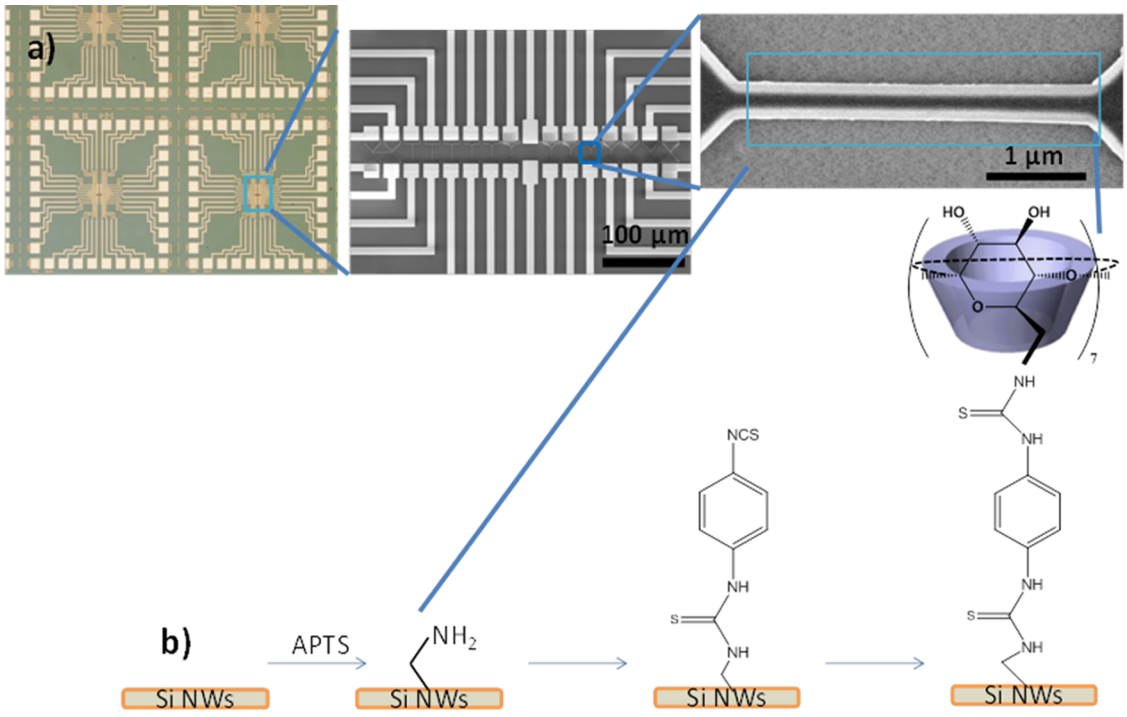

Figure 1. (a) Optical and SEM images of the Si NWFETs. (b) Process scheme of the functionalization of Si-NWs with β-CD.

be (practically) used only once, an issue that has limited this approach for applications.

Besides the covalent approach, supramolecular interactions have been of interest as an alternative strategy for (bio)molecule attachment on different surfaces due to its high specificity, controllable affinity, and reversibility.[20−22] Among all the potential candidates, β-cyclodextrin (β-CD)-based host−guest chemistry is particular attractive, since CD molecules are able to form densely packed self-assembled monolayers (SAMs) that can complex with a variety of hydrophobic organic molecules with different binding affinities.[22−26] Recently, the selective attachment of proteins to β-CD SAMs through multivalent orthogonal interactions has been reported.[27,28]

In this report we utilize the CD strategy—specifically, functionalizing a Si NWFET with β-CD SAMs—to detect small hormone molecules and proteins. Such supramolecular interfaces have the advantages of controlled attachment of (bio)molecules to the NWFET surface with respect to kinetics, thermodynamics, and orientation. In addition to homogeneous and oriented attachment, the CD strategy allows the regeneration of the nanowire surface and reuse of the functionalized devices.

Si NWFETs were fabricated from SOI wafers (Soitec) with 45 nm of boron-doped active Si layer in a lithography process similar to the ones previously described.[29] The nanowires used for the experiments are 150 nm (Figure 1a) or 1 μm wide (silicon nanoribbon type, Figure S3) and have a variable length from 1.5 to 10 μm long. The devices were covered with a passivation layer of SU-8 (an epoxy-based negative photoresist) with windows opened for the NW channel and the contact pads.

The Si NWFETs were functionalized with β-CD using a three-step procedure that is adapted from a similar procedure to prepare β-CD monolayers on silicon (Figure 1b).[30,31] First the NW surface was silanized with 3-aminopropyltriethoxysilane (APTS) through the gas phase. Subsequently, the NW was reacted with *p*-phenylenediisothiocyanate and amino-functionalized β-CD to give a β-CD monolayer (Figure 1b). Because of Debye screening,[32] a short aminosilane (APTS) was used to ensure the functionalized β-CD monolayer is close to the NW surface, to maximize the sensitivity of the NWFETs. The functionalization scheme was validated by fluorescence, ellipsometry, and water contact angle goniometry (see Supporting Information). After CD functionalization, a fluid delivery system consisting of a plastic solution chamber (mixing cell) together with a microminiature reference electrode (Harvard Apparatus) was mounted on top of bonded dies containing the Si NWFET devices. Continuous flow was used during sensing measurement (typical flow speed, 100 μL/min). These conditions ensure the fast mixing of the analytes and a stable solution gating during the sensing experiments (Supporting Information, Figure S1).

RESULTS AND DISCUSSION

To demonstrate the recognition and reversibility of the CD functionalization, the β-CD -functionalized Si NWFETs were first used to detect thyroxine enantiomers

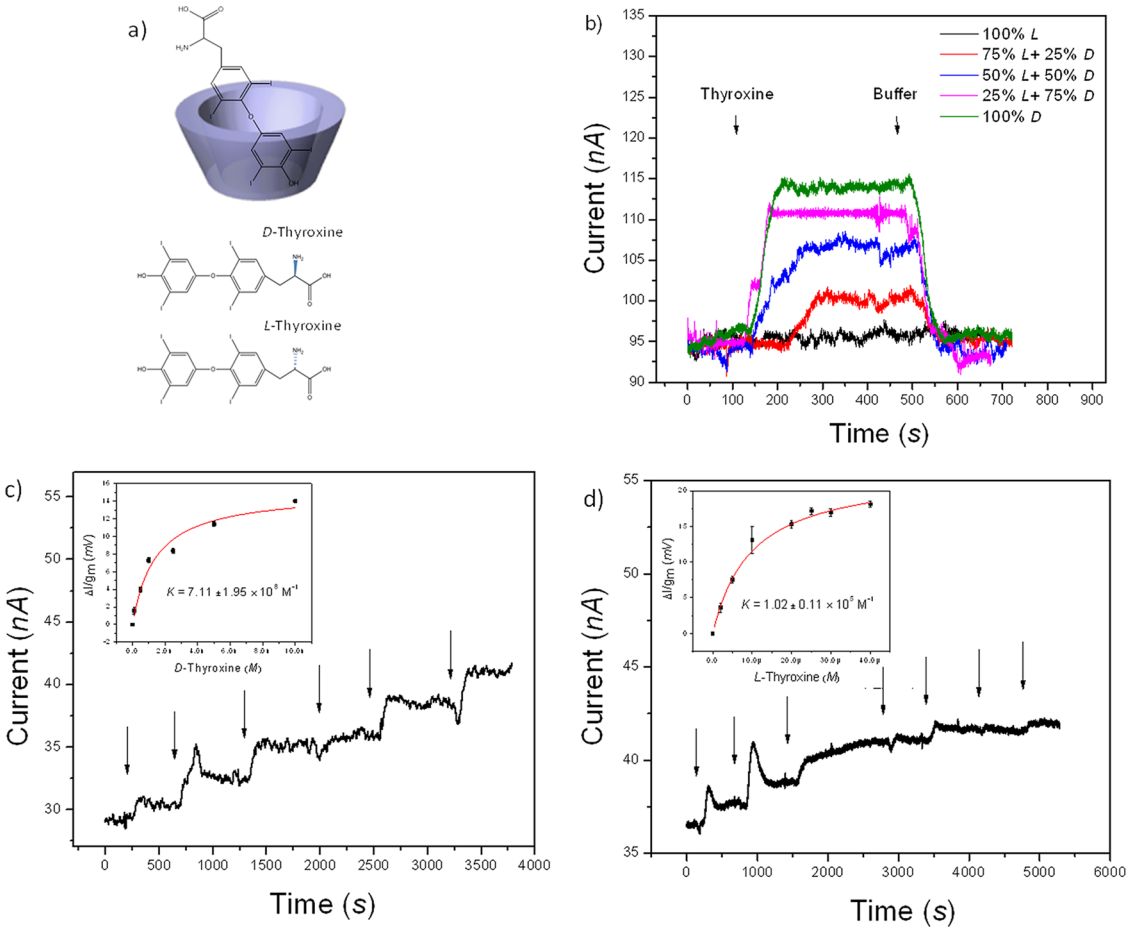

Figure 2. (a) Chemical structures of D- and L-thyroxine. (b) Real-time sensor responses of 1 nM D- and L-thyroxine and their mixtures binding and unbinding on β-CD-functionalized Si NWFETs. The real-time concentration titrations of (c) D- and (d) L-thyroxine. The arrows indicate the time at which the concentration of thyroxine is increased. Insets: Calibrated titration curve of (b) D- and (c) L-thyroxine. The error bar is obtained by the average of all data points except the transitions of each concentration. The affinity constants were obtained by fitting the titration curve with a Langmuir isotherm (red line). For all measurements 1 mM sodium carbonate buffer (pH 10.5) was used.

(Figure 2a). It is known that the biological activity of many compounds depends on their chirality, so that it is of great importance to know which compound enantiomer is present and to precisely determine the respective enantiomeric purity (*e.g.*, enantiomeric composition).[33] The two enantiomers of thyroxine (3,5,3′,5′-tetraiodothyronine) are D-thyroxine and L-thyroxine (often abbreviated as T4), the main thyroid gland hormone. Synthetically prepared L-thyroxine is used in the treatment of thyroid gland deficiency diseases; however, its counterpart D-thyroxine cannot be used for medical purposes due to cardiac side-effects.[34] Successful chiral analysis often requires a receptor molecule that can form a more stable diastereomeric complex with one of the enantiomers, and β-CDs have shown enantioselectivity in their interactions with chiral guests both in solution and on surfaces.[35−39]

Here we demonstrate that β-CD-functionalized Si NWFETs are able to discriminate between the enantiomers of thyroxine. D- and L-thyroxine solutions (1 nM) were prepared in sodium carbonate buffer (pH 10.5, 1 mM), and variable concentration ratios of the enantiomers were prepared by mixing these solutions. Figure 2b presents binding and unbinding sensograms obtained for different compositions of D- and L-thyroxine utilizing the same device. After a stable baseline was established, a solution of thyroxine was injected, and a clear increase of measured current is observed, which agrees with the negative charge of thyroxine at pH 10.5. After sensor equilibrium, the thyroxine solution was replaced by buffer and the complex was allowed to dissociate. During the experiment a return to a stable baseline was obtained, indicating the thyroxine−CD interactions are reversible and no degradation of the CD−SAM on the Si NWFETs occurs. It is also observed that the sensor responses increased with increasing percentage of the D-enantiomer, demonstrating a differential selective binding of the D- over the L-enantiomer of thyroxine on the CD-functionalized Si-NW sensor. Since the CD−thyroxine interactions are totally reversible and the sensors can be used multiple times, a "calibration curve" can be established for each chip, which means that the CD-functionalized Si-NWs can be used for the evaluation of the enantiomeric

composition of a racemic mixture of D- and L-thyroxine. To our knowledge, it is the first time that a Si NWFET was demonstrated as a chiral sensor to quantify the enantiomeric compositions. We expect that Si NWFETs can be extended to other chiral systems, suggesting that this approach could serve as a technology platform to improve drug discovery and development. Compared with other state of the art surface based biosensors such as surface plasmon resonance (SPR) and quartz crystal microbalance (QCM), the Si NWFET detects changes in surface charge density by binding of charged molecules, which has advantages over refractive index or mass detection, which is limited by the molecule weight of the analytes (typically required above 2000 g/mol when covering the surface in a monolayer fashion[40]).

Furthermore, in order to quantify the inclusion complexation behavior of the CD SAMs with the thyroxine guests, surface titration experiments (Figure 2c,d) were performed with CD-functionalized Si-nanoribbon-type devices with different concentrations of D- and L-thyroxine under the same buffer conditions. Figure 2c shows the real-time sensor responses by adding increasing concentrations of D-thyroxine. After the baseline was established, D-thyroxine solutions with concentrations of 0.1, 0.5, 1, 2.5, 5, and 10 nM (indicated by arrows in Figure 2c) were sequentially injected into the flow channel, which resulted in an increase of current owing to higher equilibrium surface coverage. The measured current change of the nanowire sensor (ΔI) was calibrated using $\Delta I/g_m$ to obtain the surface potential change,[41,42] which corresponds to the surface coverage of the thyroxine. The calibrated titration curve can be fitted by a Langmuir isotherm, using a 1:1 stoichiometry (Figure 2c, inset).[9,43] From this, we can determine an affinity constant (K) for D-thyroxine of $K = (7.11 \pm 1.95) \times 10^8\ M^{-1}$. Surface titration with L-thyroxine was performed in a similar manner (with L-thyroxine concentrations of 2, 5, 10, 20, 25, 30, and 40 μM), and the resulting curve is shown in Figure 2d. The calibrated maximum sensor response ($\Delta I/g_m$, surface potential change) is comparable with the D-thyroxine (although for much higher concentrations), which indicates the similar surface coverage of the bound thyroxine. By fitting the titration curve, the affinity constant for L-thyroxine is obtained as $K = (1.02 \pm 0.11) \times 10^5\ M^{-1}$. It is also noticed that a surprising higher affinity is obtained between the D-thyroxine and the CD−SAMs compared with its L-enantiomer (around 7000 times). Similar affinity results were reported by SPR measurement as well.[36] Such a higher affinity difference is likely due to the deep inclusion of the hydrophobic part of thyroxine in the lipophilic cavity of the cyclodextrin skeleton such that the chiral center and the polar functions of thyroxine are segregated outside the macrocycle.[35]

To demonstrate β-CD-functionalized Si NWFETs as reversible sensors for protein detection, orthogonal linkers need to be developed that contain the protein-binding ligand and guest moieties that enable linking to the β-CD SAM. The linker has to be stable during protein sensing and with the potential for stimulated desorption. Here we chose adamantane (Ad) groups as the guest sites. The Ad−β-CD interactions have been well characterized, and it was found that by choosing the correct number of Ad moieties, it is possible to control the thermodynamics, kinetics, and stoichiometry of the adsorption and desorption for such host−guest interactions.[22]

To test the stability and reversibility of the Ad−β-CD interactions, two guest molecules with either one or two Ad functionalities (which enable monovalent or divalent interactions with β-CD) were used to bind with β-CD SAMs (Figure 3a). After injection, both molecules showed rapid adsorption on CD-NWs, as shown by the increase in current, corresponding to a negatively charged layer as a result of complexation. However, the monovalent complex **1** is not stable upon rinsing with buffer (Figure 3b), whereas the divalent guest **2** is stable with buffer wash (Figure 3c). This indicates the formation of kinetically stable assemblies due to the multivalent host−guest interactions, which agrees with the previous SPR measurements.[22] We also monitored the guest molecules' adsorption through fluorescence microscopy, which was consistent with the electrical observations (Supporting Information, Figure S2). To break the kinetically stable assembly, a competitive desorption approach was employed. Compound **2** can be completely desorbed from the CD−SAM with application of 8 mM β-CD, as shown by the fully restored baseline current (Figure 3c). It is noted that from the previous SPR and fluorescent measurements desorption of the divalent molecules is normally not complete.[30] In contrast, we observed a rapid and complete desorption of the divalent guest from the Si NWFETs. Multiple adsorption and desorption cycles of compound **2** were also tested with the CD−NWs, and complete reversibility of the binding process of the divalent guest molecules could be demonstrated multiple times by the addition of β-CD (Figure 3d). The desorption process is observed to be highly selective, rapid, and reversible without compromising the performance of the Si-NWs. These results indicate that the divalent Ad groups can create stable assemblies at the CD surface that could be removed only by rinsing with a competitive β-CD solution, which is ideal as the building block of the orthogonal linker for protein sensing.

By employing this reversible, "cleavable" system, we can design a heterobifunctional cross-linker that can work with any binding affinity system, even very strong binding systems that are considered irreversible (such as biotin−streptavidin (SAv)). Here we show using this approach the detection of biotin−SAv and subsequent reversibility by removal at the β-CD SAM. An orthogonal linker **3** (Figure 4a) is developed, which

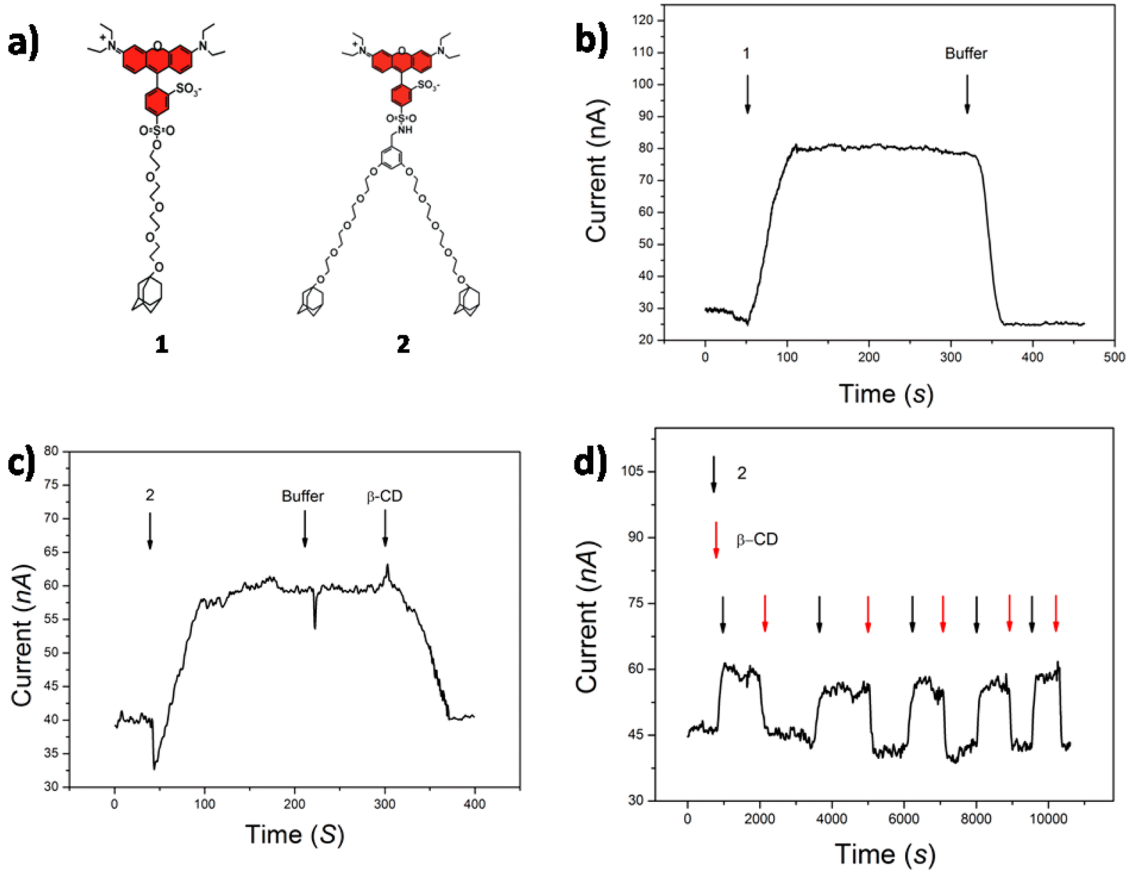

Figure 3. (a) Chemical structures of the adamantane-terminated guest compounds. Real-time sensor responses of the adsorption and desorption of (b) monovalent 1 (10 μM) and (c, d) divalent guest molecule 2 (0.1 μM) on β-CD-functionalized Si-NW FETs. For all measurements, 1 mM sodium carbonate buffer (pH 10.5) was used.

consists of two Ad functionalities to ensure stable binding to CD−NWs and a biotin functionality to ensure binding to SAv. Three oligo(ethylene glycol) (OEG) chains were incorporated in the linker to increase the solubility of the Ad groups and prevent nonspecific protein binding. An important consideration for full reversibility is appropriate control of the surface receptor density; otherwise, cleavage of the CD linker may not be efficient. For the biotin−SAv system, we found that a ~20% biotin surface density was optimal for efficient reversibility (whereas 100% coverage created a layer resistant to cleavage; see Supporting Information, Figure S4).

To achieve this density, we designed a supramolecular blocking agent, **4**, which has two Ad groups for a stable interaction with the β-CD SAMs and an OEG chain as "protein-resistant" to reduce nonspecific protein absorption. By mixing **3** and **4**, surface biotin concentration was optimized to enable SAv to form a 1:1 complex with **3**; thus the SAv is linked to β-CD SAMs through a divalent binding, which will facilitate the subsequent competitive desorption. Figure 4a shows the chemical structures of **3** and **4** and their assembly scheme on β-CD SAMs for SAv sensing.

For SAv sensing, a mixture of **3** and **4** in HEPES buffer (5 μM, ratio 1:5, pH 7.4) was adsorbed on the Si NWFET, which was experimentally confirmed by an increase in the current due to the negatively charged biotin moieties (Figure 4b). After the biotinylation, 2 nM SAv was introduced. Current increased quickly after contact with SAv, which indicates the adsorption of SAv is due to its negative charge at pH 7.4 (PI $\approx$ 5.6). After equilibration, the solution was switched to 8 mM β-CD in HEPES, and the surface-bound SAv began to desorb, which was confirmed by a decrease in the current. Since this returns to the original baseline, we conclude that the SAv desorption is almost complete. Less than 10% of the residue is left on the surface, which is likely due to the uncontrolled tetravalent binding. Further decreasing the surface biotin concentration may reduce the possibility of the tetravalent binding; however, it will also lower the signal-to-noise ratio due to the smaller coverage of SAv. As a negative control, biotin-blocked streptavidin (locked SAv) was also injected under the same conditions, and no interaction was detected (Supporting Information, Figure S5), which indicates that the sensor response proceeded only through specific interactions of SAv and surface-immobilized biotin. The demonstrated reversible binding of SAv on β-CD-functionalized Si NWFETs will allow the reuse of the β-CD-functionalized surfaces for multiple detections.

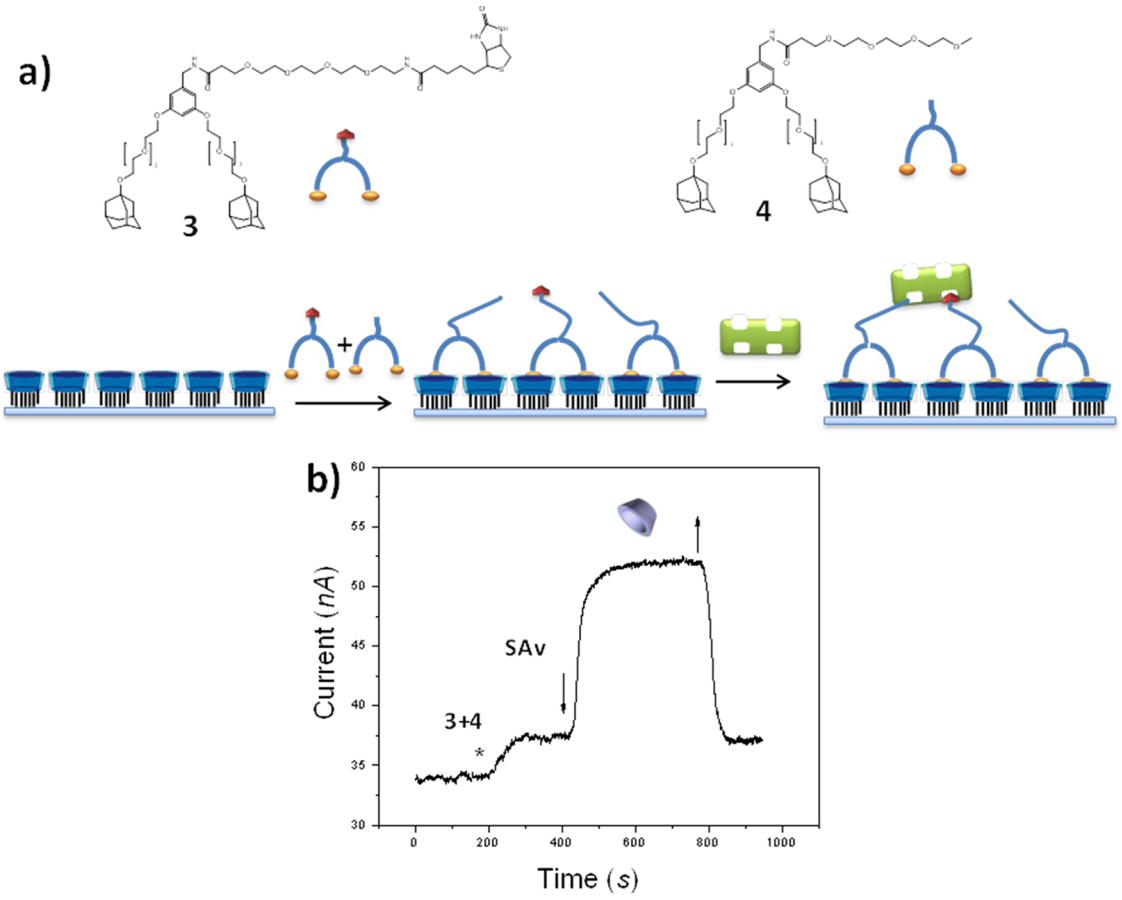

Figure 4. (a) Chemical structures of the divalent adamantyl−biotin linker 3 and adamantyl−oligo(ethylene glycol) 4 and adsorption scheme for the sensing of SAv at β-CD SAMs through a mixture of 3 and 4. (b) Real-time sensorgrams of the adsorption and desorption of 2 nM SAv through the mixture of 3 and 4 (5 μM, ratio 1:5) on β-CD-functionalized Si NWFETs. Symbols indicate switching of solutions in the flow cell: divalent linker (*), SAv (↓), and 8 mM β-CD solution (↑). For all measurements, 1 mM HEPES buffer (pH 7.4) was used.

Furthermore, the stepwise adsorption of SAv through the supramolecular linker enables the free biotin binding pockets of SAv that are directed toward the solution, which could be used for binding of other biotinylated (bio)molecules toward multidisciplinary protein detection.

CONCLUSION

In this work, we have demonstrated a supramolecular interface for Si NWFET biosensors. The Si-NWs were successfully functionalized with β-CD SAMs. These devices have been used to detect thyroxine molecules through host−guest interactions and were able to discriminate between D and L enantiomers of thyroxine, which is the first demonstration that the Si NWFETs can be used as stereoselective sensors to analyze enantiomeric compositions. β-CD-functionalized Si NWFETs were also used to detect the biotin−streptavidin interactions through small, orthogonal, multivalent linker molecules. By choosing the appropriate number and type of guest sites, it is possible to control the adsorption and desorption of molecule assemblies at such an interface. The demonstrated reversible sensing of SAv with Si NWFETs represents a versatile, promising approach for the development of regenerative electronic biosensors, which are very attractive from both a device performance and economical point of view, since it permits accurate calibration prior to measurements and repeated use of the same calibrated device.

We believe that the supramolecular interface and sensing method we developed on Si NWFETs can be used broadly in fundamental research and benefit real device applications, enhancing sensor lifetime, reliability, and repeatability.

MATERIALS AND METHODS

Materials. 3-Aminopropyltriethoxysilane (APTS), *p*-phenylene diisothiocyanate (PDC), and 4-(2-hydroxyethyl)-1-piperazineethanesulfonic acid (HEPES) were purchased from Aldrich. D-Thyroxine and L-thyroxine were ordered from MP Biomedicals LLC. EZ-Link NHS-PEG_4-biotin, and EZ-Link NHS-PEG_4 were purchased from Fisher Scientific Company LLC. All materials were used as received without further purification. Streptavidin-unconjugated

was purchased from Rockland Immunochemical. The lyophilized streptavidin was restored with deionized water and diluted to the desired concentrations with buffers before using. Per-6-amino-β-cyclodextrin, lissamine-Ad (**1**), lissamine-Ad_2 (**2**), and amino-terminated divalent adamantyl linker were synthesized at the lab of one of the authors (J.H.) according to previously published results.[27,44]

Divalent Biotin Linker and PEG Blocking Agents (3, 4). These were prepared by mixing amino-terminated divalent adamantyl linker with EZ-Link NHS-PEG_4-biotin or EZ-Link NHS-PEG_4 in DMF (1:3) (Scheme S2). The mixture was stirred at room temperature for 3 h. Subsequently, diethyl ether was added dropwise, and the product precipitated. The product was redissolved in DMF and precipitated again by adding diethyl ether dropwise.

Si Nanowire FET Biosensor Fabrications. The devices were fabricated from 4-inch SOI wafers (Soitec). The silicon active layer (p-type doping = 10^{15} cm^{-3}) was first thinned to about 45 nm by thermal oxidation, and the silicon oxide removed using wet etching (BOE Etch). The source and drain regions as well as the back-gate were patterned by contact lithography and doped by BF_2^+ implantation. Following dopant activation in a furnace at 1000 °C, the NW channels were patterned in hydrogen silsesquioxane by electron beam lithography, and for the nanoribbon devices, the 1 μm wide mesas were defined by optical lithography. The pattern was transferred through the active silicon layer using either a TMAH anisotropic wet etch (25% in H_2O at 50 °C), a Cl_2 inductively coupled plasma etch (Oxford 100), or a CF_4 reactive-ion etch (Oxford 80). The devices were then metalized by titanium/gold evaporation and patterned by lift-off. The metal contacts were annealed in a rapid thermal processor at 450 °C for 1 min, and devices were measured to ensure we had ohmic contacts. The final step was to passivate the devices with a 1 μm layer of SU8 photoresist with lithographically patterned openings at the top of the devices, the contact pads. The wafer was then hard-baked at 130 °C for 20 min.

Device Functionalization. The Si-NW oxide surfaces were cleaned with UV ozone (UV/Ozone ProCleaner Plus, Bioforce Nanosciences) for 5 min before functionalization. Then APTS was allowed to evaporate onto the SiO_2 surface through gas phase deposition for 5 h. The devices were then baked in a vacuum oven for 30 min at 120 °C. Transformation of the amino-terminated layer to an isothiocyanate-bearing layer was accomplished by exposure to a 0.01 M solution of PDC in ethanol at 40 °C for 1 h, followed by rinsing with copious amounts of ethanol and drying in a stream of nitrogen. The surface-confined β-CD layer was obtained by immersion of the isothiocyanate-covered Si-NWs in a 5 mM aqueous solution of per-6-amino-β-cyclodextrin at 40 °C for 1 h. After reaction the samples were washed with Millipore water for 5 min and rinsed with additional water to remove physisorbed material and dried in a stream of nitrogen. The rather stable CD molecules will allow the long-term storage of the functionalized sensors. We have used the same CD-modified chip for more than half a year without observing degradations of the chemical surface, whereas unprotected amine-modified chips typically last only 1 week.

Fluid Delivery System. The mixing cells (solution chamber) were created by epoxying thin-walled, ~5 mm diameter PTFE tubing to the chip surface. Microminiature reference electrodes (Harvard Apparatus) and thinner tubing (0.5 mm) serving as the fluid supply and return were inserted. The solution input tube was placed directly over the central region of the die. This system enabled continual mixing (equivalent to pippetting up and down) throughout the course of sensing measurements. In our sensing setup, different samples were pumped by a single syringe pump, and the sample exchange was achieved by using an electronically controlled solenoid valve (typical switching speed of within a second), thus maintaining a constant flow rate (100 uL/min). In these conditions, we observed no change in sensor response by switching the samples.

Conflict of Interest: The authors declare no competing financial interest.

Acknowledgment. The authors gratefully acknowledge financial support from The Netherlands Organization for Scientific Research (NWO, Rubicon grant), the National Institutes of Health (NIH R01EB008260), DTRA (HDTRA1-10-1-0037), and funded in part by the Army Research Office (MURI W911NF-11-1-0024). We are grateful to our colleagues Aleksandar Vacic, Monika Weber, and Weihua Guan for help with the electrical measurement and helpful discussions.

Supporting Information Available: The surface characterizations of β-cyclodextrin-modified device and the detection of biotin–streptavidin binding using orthogonal linker **3**. This material is available free of charge *via* the Internet at http://pubs.acs.org.

REFERENCES AND NOTES

1. Stern, E.; Vacic, A.; Reed, M. A. Semiconducting Nanowire Field-Effect Transistor Biomolecular Sensors. *IEEE Trans. Electron Devices* **2008**, *55*, 3119–3130.
2. Curreli, M.; Zhang, R.; Ishikawa, F. N.; Chang, H. K.; Cote, R. J.; Zhou, C.; Thompson, M. E. Real-Time, Label-Free Detection of Biological Entities Using Nanowire-Based FETs. *IEEE Trans. Nanotechnol.* **2008**, *7*, 651–667.
3. Elfstrom, N.; Karlstrom, A. E.; Linnros, J. Silicon Nanoribbons for Electrical Detection of Biomolecules. *Nano Lett.* **2008**, *8*, 945–949.
4. Gao, A.; Lu, N.; Dai, P.; Li, T.; Pei, H.; Gao, X.; Gong, Y.; Wang, Y.; Fan, C. Silicon-Nanowire-Based CMOS-Compatible Field-Effect Transistor Nanosensors for Ultrasensitive Electrical Detection of Nucleic Acids. *Nano Lett.* **2011**, *11*, 3974–3978.
5. Park, I.; Li, Z.; Li, X.; Pisano, A. P.; Williams, R. S. Towards the Silicon Nanowire-Based Sensor for Intracellular Biochemical Detection. *Biosens. Bioelectron.* **2007**, *22*, 2065–2070.
6. Bunimovich, Y. L.; Shin, Y. S.; Yeo, W. S.; Amori, M.; Kwong, G.; Heath, J. R. Quantitative Real-Time Measurements of DNA Hybridization with Alkylated Nonoxidized Silicon Nanowires in Electrolyte Solution. *J. Am. Chem. Soc.* **2006**, *128*, 16323–16331.
7. Zheng, G. F.; Patolsky, F.; Cui, Y.; Wang, W. U.; Lieber, C. M. Multiplexed Electrical Detection of Cancer Markers with Nanowire Sensor Arrays. *Nat. Biotechnol.* **2005**, *23*, 1294–1301.
8. Hakim, M. M. A.; Lombardini, M.; Sun, K.; Giustiniano, F.; Roach, P. L.; Davies, D. E.; Howarth, P. H.; de Planque, M. R. R.; Morgan, H.; Ashburn, P. Thin Film Polycrystalline Silicon Nanowire Biosensors. *Nano Lett.* **2012**, *12*, 1868–1872.
9. Duan, X.; Li, Y.; Rajan, N. K.; Routenberg, D. A.; Modis, Y.; Reed, M. A. Quantification of the Affinities and Kinetics of Protein Interactions Using Silicon Nanowire Biosensors. *Nat. Nanotechnol.* **2012**, *7*, 401–407.
10. Ishikawa, F. N.; Chang, H. K.; Curreli, M.; Liao, H. I.; Oison, C. A.; Chen, P. C.; Zhang, R.; Roberts, R. W.; Sun, R.; Cote, R. j.; *et al*. Label-Free, Electrical Detection of the SARS Virus N-Protein with Nanowire Biosensors Utilizing Antibody Mimics as Capture Probes. *ACS Nano* **2009**, *3*, 1219–1224.
11. Cui, Y.; Lieber, C. M. Functional Nanoscale Electronic Devices Assembled Using Silicon Nanowire Building Blocks. *Science* **2001**, *291*, 851–853.
12. Stern, E.; Klemic, J. F.; Routenberg, D. A.; Wyrembak, P. N.; Turner-Evans, D. B.; Hamilton, A. D.; LaVan, D. A.; Fahmy, T. M.; Reed, M. A. Label-Free Immunodetection with CMOS-Compatible Semiconducting Nanowires. *Nature* **2007**, *445*, 519–522.
13. Gong, J. R. Label-Free Attomolar Detection of Proteins Using Integrated Nanoelectronic and Electrokinetic Devices. *Small* **2010**, *6*, 967–973.
14. Lee, M.-H.; Lee, D.-H.; Jung, S.-W.; Lee, K.-N.; Park, Y. S.; Seong, W.-K. Measurements of Serum C-Reactive Protein Levels in Patients with Gastric Cancer and Quantification Using Silicon Nanowire Arrays. *Nanomedicine* **2010**, *6*, 78–83.
15. Stern, E.; Vacic, A.; Rajan, N. K.; Criscione, J. M.; Park, J.; Ilic, B. R.; Mooney, D. J.; Reed, M. A.; Fahmy, T. M. Label-Free Biomarker Detection from Whole Blood. *Nat. Nanotechnol.* **2010**, *5*, 138–142.

16. Fritz, J.; Cooper, E. B.; Gaudet, S.; Sorger, P. K.; Manalis, S. R. Electronic Detection of DNA by Its Intrinsic Molecular Charge. *Proc. Natl. Acad. Sci. U.S.A.* **2002**, *99*, 14142–14146.
17. Milovic, N. M.; Behr, J. R.; Godin, M.; Hou, C.-S. J.; Payer, K. R.; Chandrasekaran, A.; Russo, P. R.; Sasisekharan, R.; Manalis, S. R. Monitoring of Heparin and its Low-Molecular-Weight Analogs by Silicon Field Effect. *Proc. Natl. Acad. Sci. U.S.A.* **2006**, *103*, 13374–13379.
18. Jonkheijm, P.; Weinrich, D.; Schroder, H.; Niemeyer, C. M.; Waldmann, H. Chemical Strategies for Generating Protein Biochips. *Angew. Chem., Int. Ed.* **2008**, *47*, 9618–9647.
19. Nicu, L.; Leichle, T. Biosensors and Tools for Surface Functionalization from the Macro- to the Nanoscale: The Way Forward. *J. Appl. Phys.* **2008**, *104*, 111101–111116.
20. Mulder, A.; Huskens, J.; Reinhoudt, D. N. Multivalency in Supramolecular Chemistry and Nanofabrication. *Org. Biomol. Chem.* **2004**, *2*, 3409–3424.
21. Elemans, J.; Lei, S. B.; De Feyter, S. Molecular and Supramolecular Networks on Surfaces: From Two-Dimensional Crystal Engineering to Reactivity. *Angew. Chem., Int. Ed.* **2009**, *48*, 7298–7332.
22. Ludden, M. J. W.; Reinhoudt, D. N.; Huskens, J. Molecular Printboards: Versatile Platforms for the Creation and Positioning of Supramolecular Assemblies and Materials. *Chem. Soc. Rev.* **2006**, *35*, 1122–1134.
23. Huskens, J.; Deij, M. A.; Reinhoudt, D. N. Attachment of Molecules at a Molecular Printboard by Multiple Host-Guest Interactions. *Angew. Chem., Int. Ed.* **2002**, *41*, 4467–4471.
24. Davis, M. E.; Brewster, M. E. Cyclodextrin-Based Pharmaceutics: Past, Present and Future. *Nat. Rev. Drug Discovery* **2004**, *3*, 1023–1035.
25. Houk, K. N.; Leach, A. G.; Kim, S. P.; Zhang, X. Y. Binding Affinities of Host-Guest, Protein-Ligand, and Protein-Transition-State Complexes. *Angew. Chem., Int. Ed.* **2003**, *42*, 4872–4897.
26. Chen, Y.; Liu, Y. Cyclodextrin-Based Bioactive Supramolecular Assemblies. *Chem. Soc. Rev.* **2010**, *39*, 495–505.
27. Ludden, M. J. W.; Peter, M.; Reinhoudt, D. N.; Huskens, J. Attachment of Streptavidin to Beta-Cyclodextrin Molecutar Printboards *via* Orthogonal, Host-Guest and Protein-Ligand Interactions. *Small* **2006**, *2*, 1192–1202.
28. Ludden, M. J. W.; Mulder, A.; Tampe, R.; Reinhoudt, D. N.; Huskens, J. Molecular Printboards As a General Platform for Protein Immobilization: A Supramolecular Solution to Nonspecific Adsorption. *Angew. Chem., Int. Ed.* **2007**, *46*, 4104–4107.
29. Rajan, N. K.; Routenberg, D. A.; Chen, J.; Reed, M. A. 1/f Noise of Silicon Nanowire BioFETs. *IEEE Electron Device Lett.* **2010**, *31*, 615–617.
30. Onclin, S.; Mulder, A.; Huskens, J.; Ravoo, B. J.; Reinhoudt, D. N. Molecular Printboards: Monolayers of Beta-Cyclodextrins on Silicon Oxide Surfaces. *Langmuir* **2004**, *20*, 5460–5466.
31. Mulder, A.; Onclin, S.; Peter, M.; Hoogenboom, J. P.; Beijleveld, H.; ter Maat, J.; Garcia-Parajo, M. F.; Ravoo, B. J.; Huskens, J.; van Hulst, N. F.; *et al.* Molecular Printboards on Silicon Oxide: Lithographic Patterning of Cyclodextrin Monolayers with Multivalent, Fluorescent Guest Molecules. *Small* **2005**, *1*, 242–253.
32. Stern, E.; Wagner, R.; Sigworth, F. J.; Breaker, R.; Fahmy, T. M.; Reed, M. A. Importance of the Debye Screening Length on Nanowire Field Effect Transistor Sensors. *Nano Lett.* **2007**, *7*, 3405–3409.
33. Maier, N. M.; Franco, P.; Lindner, W. Separation of Enantiomers: Needs, Challenges, Perspectives. *J. Chromatogr. A* **2001**, *906*, 3–33.
34. Oppenheimer, J. H.; Schwartz, H. L.; Mariash, C. N.; Kinlaw, W. B.; Wong, N. C. W.; Freake, H. C. Advances in Our Understanding of Thyroid-Hormone Action at the Cellular-Level. *Endocr. Rev.* **1987**, *8*, 288–308.
35. Easton, C. J.; Lincoln, S. F. Chiral Discrimination by Modified Cyclodextrins. *Chem. Soc. Rev.* **1996**, *25*, 163–170.
36. Shahgaldian, P.; Hegner, M.; Pieles, U. A Cyclodextrin Self-Assembled Monolayer (SAM) Based Surface Plasmon Resonance (SPR) Sensor for Enantioselective Analysis of Thyroxine. *J. Inclusion Phenom. Macrocyclic Chem.* **2005**, *53*, 35–39.
37. Szejtli, J. Introduction and General Overview of Cyclodextrin Chemistry. *Chem. Rev.* **1998**, *98*, 1743–1753.
38. Kurzawski, P.; Schurig, V.; Hierlemann, A. Chiral Sensing Using a Complementary Metal-Oxide Semiconductor-Integrated Three-Transducer Microsensor System. *Anal. Chem.* **2009**, *81*, 9353–9364.
39. Kieser, B.; Fietzek, C.; Schmidt, R.; Belge, G.; Weimar, U.; Schurig, V.; Gauglitz, G. Use of a Modified Cyclodextrin Host for the Enantioselective Detection of a Halogenated Diether as Chiral Guest *via* Optical and Electrical Transducers. *Anal. Chem.* **2002**, *74*, 3005–3012.
40. Myszka, D. G. Extending the Range of Rate Constants Available from BIACORE: Interpreting Mass Transport-Influenced Binding Data. *Curr. Opin. Biotechnol.* **1997**, *8*, 50–57.
41. Ishikawa, F. N.; Curreli, M.; Chang, H. K.; Chen, P. C.; Zhang, R.; Cote, R. J.; Thompson, M. E.; Zhou, C. W. A Calibration Method for Nanowire Biosensors to Suppress Device-to-Device Variation. *ACS Nano* **2009**, *3*, 3969–3976.
42. Vacic, A.; Criscione, J. M.; Stern, E.; Rajan, N. K.; Fahmy, T.; Reed, M. A. Multiplexed SOI BioFETs. *Biosens. Bioelectron.* **2011**, *28*, 239–242.
43. Chang, H.-K.; Ishikawa, F. N.; Zhang, R.; Datar, R.; Cote, R. J.; Thompson, M. E.; Zhou, C. Rapid, Label-Free, Electrical Whole Blood Bioassay Based on Nanobiosensor Systems. *ACS Nano* **2011**, *5*, 9883–9891.
44. Ashton, P. R.; Koniger, R.; Stoddart, J. F.; Alker, D.; Harding, V. D. Amino Acid Derivatives of Beta-Cyclodextrin. *J. Org. Chem.* **1996**, *61*, 903–908.